



## King's Research Portal

### *Document Version*

Publisher's PDF, also known as Version of record

[Link to publication record in King's Research Portal](#)

### *Citation for published version (APA):*

Loru, D., Bermúdez, M., & Sanz, M. E. (2016). Structure of fenchone by broadband rotational spectroscopy. *The Journal of chemical physics*, 145, 074311. Advance online publication.

### **Citing this paper**

Please note that where the full-text provided on King's Research Portal is the Author Accepted Manuscript or Post-Print version this may differ from the final Published version. If citing, it is advised that you check and use the publisher's definitive version for pagination, volume/issue, and date of publication details. And where the final published version is provided on the Research Portal, if citing you are again advised to check the publisher's website for any subsequent corrections.

### **General rights**

Copyright and moral rights for the publications made accessible in the Research Portal are retained by the authors and/or other copyright owners and it is a condition of accessing publications that users recognize and abide by the legal requirements associated with these rights.

- Users may download and print one copy of any publication from the Research Portal for the purpose of private study or research.
- You may not further distribute the material or use it for any profit-making activity or commercial gain
- You may freely distribute the URL identifying the publication in the Research Portal

### **Take down policy**

If you believe that this document breaches copyright please contact [librarypure@kcl.ac.uk](mailto:librarypure@kcl.ac.uk) providing details, and we will remove access to the work immediately and investigate your claim.

## Structure of fenchone by broadband rotational spectroscopy

Donatella Loru, Miguel A. Bermúdez, and M. Eugenia Sanz

Citation: *The Journal of Chemical Physics* **145**, 074311 (2016); doi: 10.1063/1.4961018

View online: <http://dx.doi.org/10.1063/1.4961018>

View Table of Contents: <http://scitation.aip.org/content/aip/journal/jcp/145/7?ver=pdfcov>

Published by the AIP Publishing

---

### Articles you may be interested in

[Spectroscopic study on deuterated benzenes. I. Microwave spectra and molecular structure in the ground state](#)

*J. Chem. Phys.* **143**, 244302 (2015); 10.1063/1.4937949

[Distortion of ethyne on coordination to silver acetylide, C<sub>2</sub>H<sub>2</sub>---AgCCH, characterised by broadband rotational spectroscopy and ab initio calculations](#)

*J. Chem. Phys.* **140**, 124310 (2014); 10.1063/1.4868035

[Rotational spectroscopy and molecular structure of 1,1,2-trifluoroethylene and the 1,1,2-trifluoroethylene-hydrogen fluoride complex](#)

*J. Chem. Phys.* **126**, 114310 (2007); 10.1063/1.2710276

[Determination of structural parameters for ferrocenecarboxaldehyde using Fourier transform microwave spectroscopy](#)

*J. Chem. Phys.* **123**, 054317 (2005); 10.1063/1.1993593

[Microwave spectra, density functional theory calculations and molecular structure of acetylenemethyldioxorhenium](#)

*J. Chem. Phys.* **113**, 7891 (2000); 10.1063/1.1315611

---

The cover of the AIP Applied Physics Reviews journal. It features a blue and orange color scheme with a molecular structure background. The text 'AIP Applied Physics Reviews' is at the top left. The main title 'NEW Special Topic Sections' is in large white letters. Below it, 'NOW ONLINE' is in orange, followed by 'Lithium Niobate Properties and Applications: Reviews of Emerging Trends' in white. The AIP Applied Physics Reviews logo is at the bottom right.

## NEW Special Topic Sections

**NOW ONLINE**  
Lithium Niobate Properties and Applications:  
Reviews of Emerging Trends

**AIP** Applied Physics  
Reviews

# Structure of fenchone by broadband rotational spectroscopy

Donatella Loru, Miguel A. Bermúdez, and M. Eugenia Sanz

*Department of Chemistry, King's College London, London SE1 1DB, United Kingdom*

(Received 10 May 2016; accepted 2 August 2016; published online 19 August 2016)

The bicyclic terpenoid fenchone ( $C_{10}H_{16}O$ , 1,3,3-trimethylbicyclo[2.2.1]heptan-2-one) has been investigated by chirped pulse Fourier transform microwave spectroscopy in the 2–8 GHz frequency region. The parent species and all heavy atom isotopologues have been observed in their natural abundance. The experimental rotational constants of all isotopic species observed have been determined and used to obtain the substitution ( $r_s$ ) and effective ( $r_0$ ) structures of fenchone. Calculations at the B3LYP, M06-2X, and MP2 levels of theory with different basis sets were carried out to check their performance against experimental results. The structure of fenchone has been compared with those of norbornane (bicyclo[2.2.1]heptane) and the norbornane derivatives camphor (1,7,7-trimethylbicyclo[2.2.1]heptan-2-one) and camphene (3,3-dimethyl-2-methylenebicyclo[2.2.1]heptane), both with substituents at  $C_2$ . The structure of fenchone is remarkably similar to those of camphor and camphene. Comparison with camphor allows identification of changes in  $\angle CCC$  angles due to the different position of the methyl groups. All norbornane derivatives display similar structural changes with respect to norbornane. These changes mainly affect the bond lengths and angles of the six-membered rings, indicating that the substituent at  $C_2$  drives structural adjustments to minimise ring strain after its introduction. *Published by AIP Publishing*. [<http://dx.doi.org/10.1063/1.4961018>]

## I. INTRODUCTION

Terpenoids, formed by the aggregation of two or more isoprene (2-methylbutadiene) units, are a large class of natural products with relevance in fields such as drug development,<sup>1,2</sup> the flavour and fragrance industries,<sup>3</sup> and the environment.<sup>4</sup> Terpenoids have a wide range of biological activities, including antimicrobial, antitumor, and anti-inflammatory, and are used against diseases caused by viruses and bacteria.<sup>1,5</sup> Artemisin, used against malaria, and paclitaxel (Taxol®), used for cancer treatment, are probably the best known examples of terpenoid drugs. Due to their properties, development of new routes to synthesise terpenoids with known therapeutic activities and production of new terpenoid derivatives are bustling areas of research. Many terpenoids are produced by plants and emitted to the atmosphere, where they undergo several transformations reacting with available radicals and give rise to secondary organic aerosols (SOAs).<sup>6</sup> SOAs constitute a large fraction of organic particulate matter suspended in air and are known to contribute to air pollution and to affect the climate by producing a net cooling of the atmosphere.<sup>4,6</sup> In addition, terpenoids are volatile compounds with characteristic smells and are used as perfume ingredients.<sup>3</sup> A detailed analysis of the structure of terpenoids is essential to describe accurately their role in the biological and environmental processes in which they participate.

Here we present the structural investigation of the bicyclic monoterpene fenchone ( $C_{10}H_{16}O$ , 1,3,3-trimethylbicyclo[2.2.1]heptan-2-one, see Fig. 1) using broadband rotational spectroscopy.<sup>7</sup> Fenchone is one of

the main components of the essential oils of fennel, cedar leaf, and lavender. It has a camphoraceous sweet smell in addition to antibacterial and anticorrosive properties,<sup>8,9</sup> and so it is used as odorant in household products and as pesticide. Both natural and anthropogenic sources emit fenchone to the troposphere, where it is removed mainly through reactions with OH radicals.<sup>10</sup> Structurally, fenchone is a substituted norbornane with a ketone functional group and three additional methyl groups. Although several monoterpene derivatives have been investigated by rotational spectroscopy, such as carvone,<sup>11</sup> limonene,<sup>11</sup> thymol,<sup>12</sup> menthone,<sup>13</sup> linalool,<sup>14</sup> and others,<sup>15</sup> there is much less information on monoterpene derivatives derived from norbornane with a [2.2.1] bicyclic structure. Only the structures of camphor<sup>16</sup> ( $C_{10}H_{16}O$ , 1,7,7-trimethylbicyclo[2.2.1]heptan-2-one), an isomer of fenchone, and camphene<sup>17</sup> ( $C_{10}H_{16}$ , 3,3-dimethyl-2-methylenebicyclo[2.2.1]heptane) have been reported. Norbornanes are known for their strained bonds and angles, as they are constrained to have the cyclohexane ring in an envelope configuration, which gives rise to high reactivity.<sup>18</sup> Determining the structure of fenchone is relevant to model properly its interactions with other molecules and its kinetics, and it can shed light on the strains and reaction outcomes of substituted norbornanes.

Rotational spectroscopy is a powerful structural technique, able to discriminate minute changes in mass distribution and yield positive identifications of conformers and tautomers of a wide range of molecular systems.<sup>19–21</sup> In this work broadband rotational spectroscopy<sup>7</sup> has been used to characterise the structure of fenchone. With this

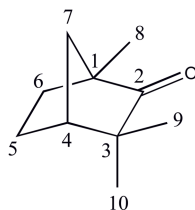


FIG. 1. Scheme of the molecular structure of fenchone and numbering of the carbon atoms.

technique, large portions of the rotational spectrum of a molecule can be collected at once, which facilitates the identification of spectral patterns and reduces acquisition time. It also aids the observation of isotopologues in their natural abundance if the rotational spectrum is sufficiently intense. Analysis of the data obtained from the rotational spectrum leads to the determination of experimental bond lengths and angles, which can then be compared with theoretically predicted ones to benchmark theoretical methods.<sup>22</sup>

The bicyclic structure of fenchone does not allow for torsional flexibility and therefore fenchone is expected to present one conformation. Examination of the rotational spectrum of fenchone led to the identification of transitions corresponding to the parent and all heavy atom isotopologues and confirmed the presence of only one structure. No splittings due to the internal rotation of the methyl groups of fenchone have been observed in its rotational spectrum. The height of the internal rotation barriers has been investigated theoretically and found to be in agreement with observations. The rotational constants of all observed species have been used to determine the substitution ( $r_s$ ) and effective ( $r_0$ ) structures of fenchone. These structures have been compared with those calculated by theoretical methods and with the crystal structure of fenchone obtained by X-ray diffraction.<sup>23</sup> Our results are also compared with those obtained for related terpenoids.

## II. EXPERIMENTAL

The rotational spectrum of fenchone was recorded using our chirped-pulse Fourier transform microwave spectrometer at King's College London, which operates in the 2-8 GHz frequency range. The design of the instrument (see scheme in Fig. 2) basically follows that previously described by Neill *et al.*<sup>24</sup>

In our spectrometer microwave excitation chirped pulses, varying linearly in frequency from 2 to 8 GHz and spanning 1-5  $\mu$ s, are created by a 24 GS/s arbitrary waveform generator (Tektronix AWG 7122C). The chirped pulse power is controlled by variable attenuators (Agilent 8494B), input into a 200 W pulsed travelling wave tube amplifier (TWTA, IFI GT82-200), and broadcast into the vacuum chamber using standard horn antennas (A-INFO LB-2060-H) separated approximately 40 cm.

In the vacuum chamber the microwave pulse interacts with the a supersonic jet of our sample molecules seeded

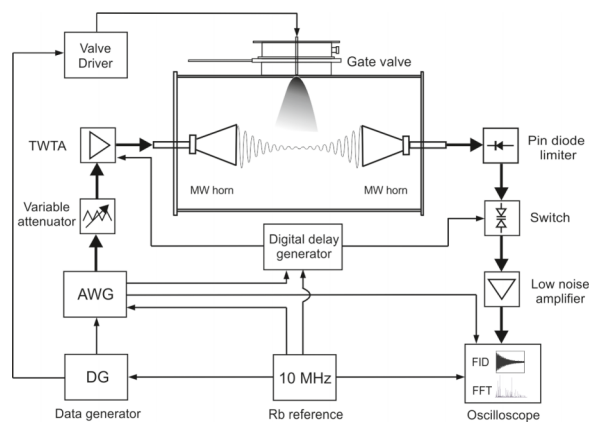


FIG. 2. Scheme of the 2-8 GHz broadband rotational spectrometer at King's College London. Thick lines indicate microwave radiation.

in a carrier gas, which is formed after expansion through a solenoid valve of 1 mm diameter (General Valve series 9). The valve is actuated by a valve driver (IOTA ONE, Parker Hannifin), triggered by a data generator (Tektronix DG2040) which also triggers the arbitrary waveform generator. Once the microwave radiation stops, the molecular emission signal is collected by the second horn antenna, amplified by a low noise amplifier (CIAO wireless, CA28-4441B), and digitised in the time domain by a 100 GS/s oscilloscope (Tektronix DPO71604C). The detection branch of the electronics is protected from accidental damage by a pin diode (Advanced Control Components ACLM-4540) and a microwave switch (Advanced Control Components S1S3R) positioned in front of the low noise amplifier. All frequency and trigger sources as well as the digital oscilloscope are phase locked to a 10 MHz rubidium frequency standard (SRS FS725).

Fenchone (Sigma-Aldrich, 98%) was used without any further purification. It is a liquid at room temperature with low vapour pressure (1 mm Hg at 301 K), and so gentle heating was used to increase the concentration of the sample in the gas phase. Fenchone was placed in a bespoke heating reservoir attached to the nozzle. The optimal temperature for vaporisation was determined by performing tests at different temperatures monitoring the intensity of the spectrum (see Fig. 3), and it was found to be ca. 343 K.

Vaporised fenchone was seeded in neon at backing pressures of ca. 5 bars. Typically molecular pulses of 1100  $\mu$ s were used to produce the supersonic jet of fenchone in our vacuum chamber. Microwave chirped pulses of 4  $\mu$ s were applied with a delay of 1400  $\mu$ s with respect to the start of the molecular pulse. Molecular relaxation signals were collected for 15  $\mu$ s using the digital oscilloscope and converted into the frequency domain through a fast Fourier-transform algorithm using a Kaiser-Bessel window. The microwave radiation is perpendicular to the supersonic jet in our setup, and therefore the transit time of the molecules through the interacting region with the radiation is short, which results in lines with FWHM  $\sim$ 110 kHz with the settings above.

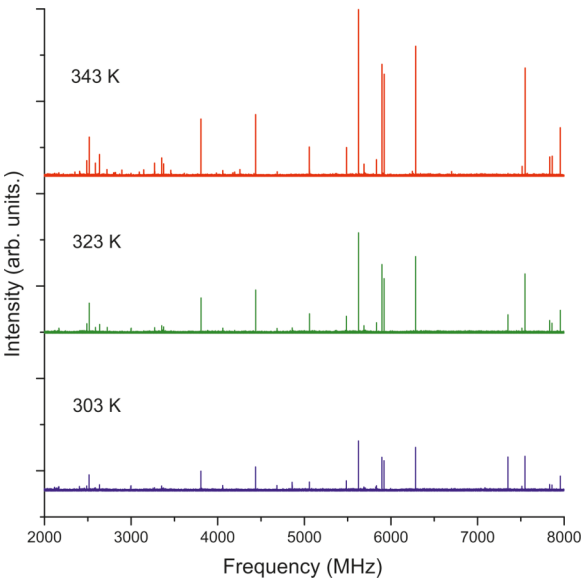


FIG. 3. Broadband rotational spectra of fenchone (500 FIDs) collected at 303 K, 323 K, and 343 K. All traces have the same scale in the  $y$  axis.

III. RESULTS

A. Rotational spectrum

The broadband rotational spectrum of fenchone in the 2-8 GHz frequency region (see Figs. 3 and 4) shows several very prominent lines and hundreds of less intense lines that are revealed when the spectrum is magnified. Fenchone is a highly asymmetric top, with the main component of the dipole moment expected to lie along the  $b$  inertial axes, and therefore we first looked for R-branch  $b$ -type transitions of the series  $J'_{1,J'} \leftarrow J''_{0,J''}$  and  $J'_{0,J'} \leftarrow J''_{1,J''}$ . The  $J'_{1,J'} \leftarrow J''_{0,J''}$  and  $J'_{0,J'} \leftarrow J''_{1,J''}$  transitions are separated by approximately  $2C$  and  $2B$ , respectively, although considering the asymmetry of fenchone we expected these separations to hold only loosely and for low  $J$  transitions.<sup>25</sup> Once these lines were identified (see Fig. 4) and fitted to yield an initial set of rotational constants, further prediction and measurement of transitions confirmed the original assignment. The final set of measured

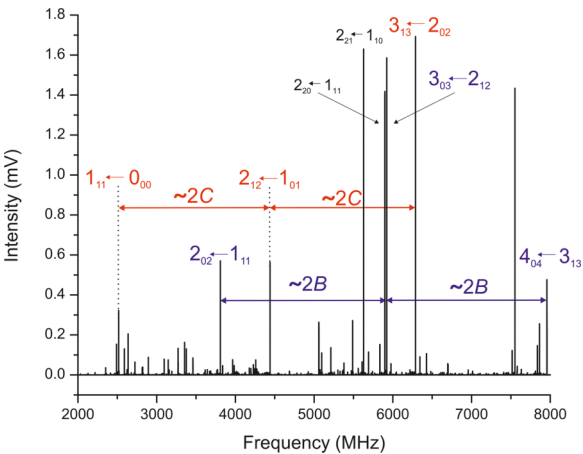


FIG. 4. Broadband rotational spectrum of fenchone (300k FIDs) in the 2-8 GHz frequency region.

$a$ -,  $b$ -, and  $c$ -type transitions (Table S1 of the [supplementary material](#)) were fit using the Watson Hamiltonian in the A reduction and I' representation<sup>26</sup> and Pickett's program<sup>27</sup> to give the rotational and quartic centrifugal distortion constants in Table I. The centrifugal distortion constants are quite small, which is an indication of the rigidity of fenchone. Similar values of the centrifugal distortion constants have been obtained for the related terpenoids camphor<sup>16</sup> and camphene.<sup>17</sup>

The experimental rotational constants can be compared with those predicted from theory to benchmark performance. Geometry optimizations of fenchone were carried out using density functional theory, with the B3LYP and M06-2X functionals, and *ab initio* calculations using the Moller-Plesset perturbation theory to second order (MP2). Pople's 6-311G++(d,p) basis set and the Dunning basis sets cc-pVTZ and aug-cc-pVTZ were used with all methods. From the data in Table II, the best agreement with the experimental rotational constants is provided by calculations at the MP2/6-311++G(d,p) level.

Many transitions of fenchone have S/N ratios of 1000/1 and above and show a number of lines at lower frequencies with about one hundredth of the intensity (see Fig. 5). These lines were identified as belonging to the ten possible <sup>13</sup>C isotopologues and the <sup>18</sup>O isotopologue in their natural abundance (1.1% and 0.2%, respectively). For all of them  $b$ - and  $c$ -type transitions were measured (see Tables S2-S12 in the [supplementary material](#)) and fitted using the same procedure as for the parent species to yield the rotational constants in Table III. In all fits the centrifugal distortion constants were fixed to those determined for parent fenchone.

Fenchone presents three non-equivalent methyl groups, which can potentially produce splittings in the rotational transitions through the coupling of their internal rotation to the overall rotation. No splittings due to internal rotation were observed in the spectrum of fenchone, suggesting that the barriers hindering internal rotation were relatively high. This was further confirmed by performing scans of the relevant

TABLE I. Experimental spectroscopic constants of fenchone.

Parameter	
A <sup>a</sup> (MHz)	1555.750 82(27) <sup>b</sup>
B (MHz)	1168.264 37(25)
C (MHz)	961.419 07(25)
$\Delta_J$ (kHz)	0.0343(69)
$\Delta_{JK}$ (kHz)	-0.0312
$\Delta_K$ (kHz)	0.0387(32)
$\delta_J$ (kHz)	0.00467(36)
$\delta_K$ (kHz)	0.0448(30)
$a/b/c$ (D)	y/y/y
$\sigma^d$ (kHz)	4.7
N <sup>e</sup>	150

<sup>a</sup>A, B, and C are the rotational constants;  $\Delta_J$ ,  $\Delta_{JK}$ ,  $\Delta_K$ ,  $\delta_J$ , and  $\delta_K$  are the centrifugal distortion constants.

<sup>b</sup>Standard error in parentheses in units of the last digit.

<sup>c</sup>Yes (y) or no (n) observation of  $a$ -,  $b$ -, and  $c$ -type transitions.

<sup>d</sup> $\sigma$  is the rms deviation of the fit.

<sup>e</sup>N is the number of the fitted transitions.



TABLE II. Calculated spectroscopic parameters of fenchone.

Parameter	6-311++G(d,p)					
	MP2		B3LYP		M062X	
A <sup>a</sup> (MHz)	1558.5	0.2% <sup>b</sup>	1551.2	−0.5%	1563.4	0.8%
B (MHz)	1172.2	0.3%	1157.0	−1.0%	1175.9	0.8%
C (MHz)	964.5	0.3%	955.1	−0.6%	966.7	0.5%
$\mu_a/\mu_b/\mu_c$ (D)	0.1/2.5/1.2		0.2/2.8/1.2		0.1/2.8/1.1	

Parameter	Cc-pVTZ					
	MP2		B3LYP		M062X	
A <sup>a</sup> (MHz)	1568.1	0.8% <sup>b</sup>	1558.2	0.2%	1569.3	0.9%
B (MHz)	1182.4	0.9%	1162.3	−0.5%	1181.1	1.1%
C (MHz)	971.5	0.7%	959.4	−0.2%	970.9	1.0%
$\mu_a/\mu_b/\mu_c$ (D)	0.1/2.5/1.0		0.1/2.6/1.1		0.1/2.7/1.1	

Parameter	Aug-cc-pVTZ					
	MP2		B3LYP		M062X	
A <sup>a</sup> (MHz)	1566.8	0.7% <sup>b</sup>	1558.3	0.2%	1570.0	0.9%
B (MHz)	1181.7	1.1%	1162.0	−0.5%	1180.6	1.1%
C (MHz)	971.2	1.0%	959.1	−0.2%	970.7	1.0%
$\mu_a/\mu_b/\mu_c$ (D)	0.1/2.7/1.1		0.1/2.8/1.2		0.1/2.8/1.1	

<sup>a</sup>A, B, and C are the rotational constants.<sup>b</sup>Deviation from the experiment; calculated as  $(A_{\text{calc}} - A_{\text{exp}})/A_{\text{exp}} \times 100\%$ .<sup>c</sup> $\mu_a$ ,  $\mu_b$ , and  $\mu_c$  are the electric dipole moment components along the principal inertial axes.

dihedral angles for the rotation of the methyl groups at the MP2/6-311++(d,p) level of theory (see Fig. S1 in the [supplementary material](#)). The barrier heights obtained were of  $900 \text{ cm}^{-1}$  ( $10.8 \text{ kJ mol}^{-1}$ ),  $1000 \text{ cm}^{-1}$  ( $12.0 \text{ kJ mol}^{-1}$ ), and  $1150 \text{ cm}^{-1}$  ( $13.8 \text{ kJ mol}^{-1}$ ), for the C<sub>8</sub>, C<sub>9</sub>, and C<sub>10</sub> methyl groups, respectively. The methyl group internal rotational splittings predicted with these barriers, using the program XIAM,<sup>28</sup> are smaller than 1 kHz and therefore not resolvable in our experiment. Related molecules such as camphor,<sup>16</sup>  $\alpha$ - and  $\beta$ -pinene,<sup>29</sup> and nopinone,<sup>29</sup> with similar predicted

methyl internal rotation barriers, do not show internal rotation splittings in their spectra.

## B. Structural determination

The determined rotational constants for the parent and all <sup>13</sup>C and <sup>18</sup>O isotopic species of fenchone allowed the calculation of the coordinates of all heavy atoms using Kraitchman's equations<sup>30</sup> and the program KRA.<sup>31</sup> Two of the carbon atoms are positioned close to one of the principal axes, returning imaginary values of the coordinates after applying Kraitchman's equations. Specifically, these were the *a* coordinate of C<sub>2</sub> and the *b* coordinate of C<sub>3</sub>. In these cases the values of the coordinates have been set to zero to determine structural parameters. The coordinates (see Table S13 in the [supplementary material](#)), all of them carrying Costain's error<sup>32</sup> to give a better account of vibration-rotation effects, were used to obtain the substitution (*r<sub>s</sub>*) structure of Table IV. Since Kraitchman's equations only provide the absolute value of the coordinates, the signs were taken from *ab initio* calculations. The signs of atomic coordinates were consistent across all theoretical methods and basis sets used, except for the *b* coordinate of C<sub>3</sub>, which is calculated to range between  $-0.0023$  and  $+0.0035$  and was set to zero to determine the substitution structure.

Given the limitations of the Kraitchman analysis, the effective structure *r<sub>0</sub>* of fenchone has also been determined through least-squares fit of the experimental moments of inertia of the observed isotopologues using the program STRFIT.<sup>31</sup> With the rotational constants of all isotopologues of the heavy atom framework, it is possible to determine the

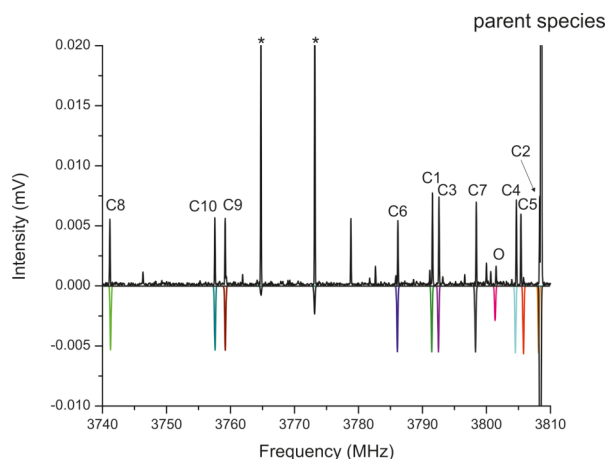


FIG. 5. Rotational spectrum of fenchone from 3740 to 3810 MHz. The figure shows the lines corresponding to the  $2_{0,2} \leftarrow 1_{1,1}$  transition of the parent species and <sup>13</sup>C and <sup>18</sup>O isotopologues in natural abundance. The asterisks indicate other transitions of the parent species.

TABLE III. Experimental spectroscopic constants for the  $^{13}\text{C}$  and  $^{18}\text{O}$  isotopologues of fenchone.

	$^{13}\text{C}_1$	$^{13}\text{C}_2$	$^{13}\text{C}_3$	$^{13}\text{C}_4$	$^{13}\text{C}_5$	$^{13}\text{C}_6$
A <sup>a</sup> (MHz)	1555.615 50(41) <sup>b</sup>	1551.525 15(29)	1555.760 85(26)	1546.446 69(37)	1535.945 82(24)	1547.237 00(32)
B (MHz)	1164.060 11(37)	1168.169 27(25)	1164.324 14(22)	1166.654 57(31)	1167.386 03(22)	1160.970 96(25)
C (MHz)	958.560 72(41)	959.948 99(25)	958.768 37(25)	958.159 37(31)	954.196 02(22)	956.378 57(28)
$\sigma^c$ (kHz)	6.5	4.6	4.6	5.9	4.2	5.4
N <sup>d</sup>	27	29	33	30	31	32
	$^{13}\text{C}_7$	$^{13}\text{C}_8$	$^{13}\text{C}_9$	$^{13}\text{C}_{10}$	$^{18}\text{O}$	
A (MHz)	1545.305 80(25)	1550.580 04(25)	1546.965 84(30)	1549.680 69(28)	1513.310 97(77)	
B (MHz)	1161.923 77(19)	1151.650 01(21)	1153.118 48(25)	1153.100 27(24)	1165.593 49(50)	
C (MHz)	959.663 12(21)	948.432 31(22)	952.931 66(25)	953.266 70(24)	946.747 44(57)	
$\sigma$ (kHz)	4.1	4.1	4.8	4.5	5.7	
N	31	30	30	30	14	

<sup>a</sup>A, B, and C are the rotational constants. The centrifugal distortion constants were fixed to the values obtained for the parent species.<sup>b</sup>Standard error in parentheses in units of the last digit.<sup>c</sup> $\sigma$  is the rms deviation of the fit.<sup>d</sup>N is the number of fitted transitions.

internal coordinates of these atoms, 27 parameters in total (10 bond lengths, 9 angles, and 8 dihedral angles), also shown in Table IV. The non-floated parameters of the hydrogen atoms were fixed at the values predicted by MP2/6-311++G(d,p) theory. The fit has a standard deviation of  $0.0092 \text{ u}\text{\AA}^2$  and returns relatively large uncertainties for the distances of  $r(\text{C}_2\text{—C}_3)$  and  $r(\text{C}_3\text{—C}_4)$ , and the  $\angle\text{OC}_2\text{C}_3$  and  $\angle\text{C}_{10}\text{C}_3\text{C}_4$  (see Table IV). Adopting a planar structure around the carbonyl group, a strategy followed for the related terpenoid camphor,<sup>16</sup> did not help improve the quality of the fit. Reducing the number of floating parameters decreases the standard deviation of the fit, at the expense of including more theoretically predicted internal coordinates, but the values of the floated parameters remain essentially the same. Several fits to determine the mass-dependent structure  $r_m$ , which is usually close to the equilibrium structure, were also attempted. However, none of the parameters that account for the isotope-dependent rovibrational contributions to the moments of inertia<sup>33</sup> could be determined.

The experimental  $r_s$  and  $r_0$  structural parameters are in good agreement, and they correspond well with the  $r_e$  equilibrium bond lengths and angles (see Table IV). A comparison between the substitution structure and the *ab initio* MP2 structure, showing the fine match of the experimental and predicted atomic coordinates, is shown in Fig. 6. Several  $r_0$  and MP2 bond lengths and angles, discussed below, are also indicated in Fig. 6. There are a few discrepancies between the  $r_s$  and  $r_0$  structures, mainly in the values of the bond lengths involving  $\text{C}_3$  and the carbons of the methyl groups attached to it. Specifically, the substitution distance  $r(\text{C}_9\text{—C}_3)$  is quite long while  $r(\text{C}_{10}\text{—C}_3)$  is very short. There are also some differences between the  $r_s$  and  $r_0$  values of the bond lengths in which atom  $\text{C}_1$  is involved. In both cases, the  $r_0$  values are closer to the theoretically predicted ones, and they are also closer to the experimental bond lengths determined for camphor.<sup>16</sup> The proximity of  $\text{C}_1$  and  $\text{C}_3$  to two principal inertial axes (their  $b$  and  $c$  coordinates are quite small (see Table S13), and the  $b$  coordinate of  $\text{C}_3$  had to be fixed to zero to determine the  $r_s$  structure) is likely to be the cause of these differences,

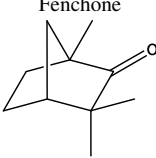
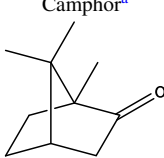
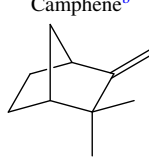

and therefore the  $r_s$  structural parameters for these two atoms should be taken with reservation. The  $r_s$  and  $r_0$  bond lengths for the  $\text{C=O}$  are basically identical, and they are extremely close to the theoretical  $r_e(\text{C=O})$  bond lengths. Finally, a relatively short  $r_0(\text{C}_8\text{—C}_1)$  is obtained, which is predicted theoretically with similar values at all levels of theory.

#### IV. DISCUSSION

The structure of fenchone had been previously studied using X-ray crystallography,<sup>23</sup> and the parameters obtained are displayed alongside the  $r_s$ ,  $r_0$ , and  $r_e$  structures determined in this work in Table IV. The values of the X-ray structure differ from the gas phase ones mainly on the distances  $r(\text{C}_3\text{—C}_4)$  and  $r(\text{C}_5\text{—C}_6)$ , and the dihedral angles  $\tau(\text{C}_3\text{C}_4\text{C}_5\text{C}_6)$ ,  $\tau(\text{C}_4\text{C}_5\text{C}_6\text{C}_1)$  and  $\tau(\text{C}_8\text{C}_1\text{C}_6\text{C}_5)$ . It should be noted that on average the bond distances in the crystal are about  $0.007 \text{ \AA}$  shorter than the  $r_0$  structure. This may be due to the effect of packing forces in the crystal.

The structure of fenchone shows many features common to other bicyclo[2.2.1]heptane derivatives, whose figures and structural parameters are collected in Table IV. In the following discussion we will consider the  $r_0$  structures of all derivatives as the  $r_s$  structures present some limitations. The  $r_0$  parameters obtained for fenchone are in excellent agreement with those determined for the related monoterpenoids camphor<sup>16</sup> and camphene.<sup>17</sup> Most bond distances and angles have effectively the same values, considering their uncertainties. Specifically, the  $\text{C=O}$  bond lengths in camphor and fenchone show an extremely good match, and the same occurs with the unusually short distance  $\text{C}_8\text{—C}_1$  involving the methyl substituent at  $\text{C}_1$ . The changes in the methyl group positions in going from camphor to fenchone do not seem to affect the carbon-carbon distances within the bicyclic ring, confirming its rigidity. The only exceptions are the angles  $\angle\text{C}_3\text{C}_4\text{C}_5$ , which is more acute (by ca.  $4^\circ$ ) in camphor than in fenchone and camphene, and  $\angle\text{C}_7\text{C}_1\text{C}_6$ , which is more obtuse by ca.  $2^\circ$  in camphor than in fenchone and camphene. This is

TABLE IV. Comparison of the bond lengths (in Å) and angles (in degrees) of the heavy atoms of fenchone determined experimentally and theoretically, and with those of related molecules.

	Fenchone				Camphor <sup>a</sup>		Camphene <sup>b</sup>	Norbornane <sup>c</sup>
								
	$r_s$	$r_0^d$	X-ray <sup>e</sup>	MP2				
$r(\text{C}_1\text{—C}_6)$	1.521(13)	1.555(18)	1.550(6)	1.559	1.557(6)	1.556(5)	1.536(15)	1.536(15)
$r(\text{C}_1\text{—C}_2)$	1.512(11)	1.526(29) <sup>f</sup>	1.517(5)	1.522	1.537(10)	1.510(8)	1.536(15)	1.536(15)
$r(\text{C}_2\text{—C}_3)$	1.545(14)	1.535(31)	1.526(5)	1.538	1.530(3)	1.527(5)	1.573(15)	1.573(15)
$r(\text{C}_3\text{—C}_4)$	1.565(17)	1.549(30)	1.517(5)	1.550	1.545(5)	1.555(7)	1.536(15)	1.536(15)
$r(\text{C}_4\text{—C}_5)$	1.531(4)	1.546(8)	1.537(5)	1.541	1.547(4)	1.546(6)	1.536(15)	1.536(15)
$r(\text{C}_5\text{—C}_6)$	1.566(5)	1.562(9)	1.542(6)	1.557	1.564(6)	1.562(5)	1.573(15)	1.573(15)
$r(\text{C}_7\text{—C}_1)$	1.536(13)	1.541(25)	1.547(6)	1.541	1.543(8)	1.544(6)	1.546(24)	1.546(24)
$r(\text{C}_7\text{—C}_4)$	1.541(3)	1.552(8) <sup>f</sup>	1.547(6)	1.544	1.555(8)	1.550(7)	1.546(24)	1.546(24)
$r(\text{C}_8\text{—C}_1)$	1.537(7)	1.521(11)	1.518(6)	1.513	1.522(4)	...	...	...
$r(\text{C}_9\text{—C}_3)$	1.568(18)	1.545(16)	1.538(6)	1.537	...	1.541(10)	...	...
$r(\text{C}_{10}\text{—C}_3)$	1.504(18)	1.535(13)	1.524(5)	1.531	...	1.543(12)	...	...
$r(\text{O—C}_2)$	1.213(3)	1.214(5)	1.215(4)	1.218	1.212(2)	...	...	...
$r(\text{C}_2\text{=C})$	...	...	...	...	...	1.340(6)	...	...
$\angle(\text{C}_1\text{C}_6\text{C}_5)$	103.6(3)	103.9(7)	104.5(3)	104.30	103.8(3)	103.1(3)	102.71	102.71
$\angle(\text{C}_1\text{C}_2\text{C}_3)$	107.2(7)	107.5(12) <sup>f</sup>	107.6(3)	107.5	105.8(2)	106.9(5)	102.71	102.71
$\angle(\text{C}_2\text{C}_3\text{C}_4)$	99.7(4)	100.8(9)	101.0(3)	100.70	101.6(1)	101.1(4)	102.71	102.71
$\angle(\text{C}_3\text{C}_4\text{C}_5)$	109.3(8)	110.3(8)	110.4(3)	110.37	106.5(3)	110.8(6)	108.97	108.97
$\angle(\text{C}_4\text{C}_5\text{C}_6)$	102.46(15)	102.8(3)	102.9(3)	102.69	102.6(1)	103.1(3)	102.71	102.71
$\angle(\text{C}_7\text{C}_1\text{C}_6)$	103.0(7)	101.4(11)	101.2(3)	100.76	103.0(6)	101.1(3)	102.04(6)	102.04(6)
$\angle(\text{OC}_2\text{C}_3)$	124.5(13)	125.8(31)	125.8(3)	125.53	126.8(1)	126.7(3)	...	...
$\angle(\text{C}_8\text{C}_1\text{C}_6)$	115.9(5)	115.3(11)	115.4(3)	115.29	114.8(3)	...	...	...
$\angle(\text{C}_9\text{C}_3\text{C}_4)$	109.6(13)	111.4(14)	110.8(3)	111.43	...	110.2(9)	...	...
$\angle(\text{C}_{10}\text{C}_3\text{C}_4)$	117.4(13)	116.2(22)	115.9(3)	115.91	...	113.9(6)	...	...
$\angle(\text{C}_1\text{C}_7\text{C}_4)$	94.4(3)	95.2(6) <sup>f</sup>	95.2(3)	95.6	94.5(4)	94.2(2)	93.41(9)	93.41(9)
$\tau(\text{C}_2\text{C}_3\text{C}_4\text{C}_5)$	72.3(11)	70.2(13)	70.4(4)	70.2	...	...	...	...
$\tau(\text{C}_3\text{C}_4\text{C}_5\text{C}_6)$	−68.1(5)	−67.3(10)	−65.3(4)	−67.2	...	...	...	...
$\tau(\text{C}_4\text{C}_5\text{C}_6\text{C}_1)$	−5.7(5)	−5.9(9)	−7.8(4)	−6.1	...	...	...	...
$\tau(\text{C}_7\text{C}_1\text{C}_6\text{C}_5)$	−30.3(4)	−30.3(7)	−28.5(4)	−29.9	...	...	...	...
$\tau(\text{C}_8\text{C}_1\text{C}_6\text{C}_5)$	−161.0(7)	−160.6(16)	−158.0(3)	−161.4	...	...	...	...
$\tau(\text{C}_9\text{C}_3\text{C}_4\text{C}_7)$	79.8(6)	80.4(11)	81.4(4)	80.6	...	...	...	...
$\tau(\text{C}_{10}\text{C}_3\text{C}_4\text{C}_2)$	−122.2(18)	−119.7(15)	...	−119.0	...	...	...	...
$\tau(\text{OC}_2\text{C}_3\text{C}_4)$	−178.3(6)	−177.7(10)	−178.9(4)	−177.5	...	...	...	...

<sup>a</sup>Reference 16.<sup>b</sup>Reference 17.<sup>c</sup>Reference 34.<sup>d</sup>Non-fitted parameters were fixed to the MP2/6-311++G(d,p) values.<sup>e</sup>Reference 23.<sup>f</sup>These parameters were not fitted directly using STRFIT but derived from the obtained  $r_0$  structure.

likely to be related to the absence of methyl groups at  $\text{C}_3$  and their presence at  $\text{C}_7$  in camphor.

Fenchone, camphor and camphene are all norbornane derivatives, and their structural parameters can be examined with relation to those of norbornane<sup>34</sup> (see Table IV). Norbornane is an archetypical molecule for strained bond lengths and angles. The bicyclic skeleton of norbornane forces the six-membered ring into a boat configuration and results in angles considerably smaller than those usually found for singly bonded ( $\text{sp}^3$ ) carbon atoms, and C—C bonds longer or shorter than the typical C—C bond length. In particular, the angle involving the bridge carbon  $\text{C}_7$  is quite strained, with a value of  $93.41(9)^\circ$ . Due to its  $\text{C}_{2v}$  symmetry, norbornane

has three different C—C bond lengths (see Table IV). In going from norbornane to camphene, camphor and fenchone, the most important change is the addition of an unsaturated substituent ( $=\text{CH}_2$ ) or a carbonyl group ( $=\text{O}$ ) at  $\text{C}_2$ , thereby modifying the character of the  $\text{C}_2$  carbon and giving rise to significant structural adjustments. The most drastic effect occurs on the  $\text{C}_2\text{—C}_3$  bond length, which is reduced by ca. 3% from 1.573(15) Å in norbornane to values around 1.530 Å in the three norbornane derivatives. Other bond lengths in the six-membered rings of fenchone, camphor, and camphene are also modified: the  $\text{C}_5\text{—C}_6$  bond length also decreases, but to a much lesser extent (ca. 0.7%); the  $\text{C}_1\text{—C}_6$ ,  $\text{C}_3\text{—C}_4$ , and  $\text{C}_4\text{—C}_5$  bonds are elongated by about 1%, with very



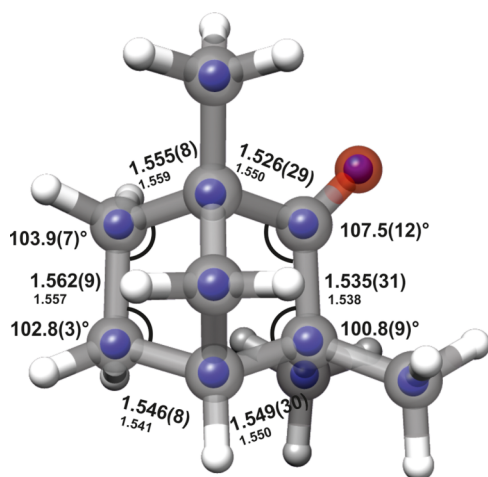


FIG. 6. Comparison of the *ab initio* MP2 structure of fenchone (full molecular drawing) with the  $r_s$  atom coordinates (the blue spheres represent the C atoms and the purple sphere represents the O atom, all from Kraitchman analysis). The  $r_0$  (top) and MP2 (bottom) values of selected bond lengths (in Å) and angles of fenchone are also indicated on the figure.

similar values for the three substituted [2.2.1] bicyclic monoterpenoids; the  $C_1$ — $C_2$  bond is shortened by about 2% in camphene, while it is basically unchanged for fenchone and camphor, a reflection of the different  $C_2$  substituent. In contrast, the bond lengths involving the bridge carbon  $C_7$  do not suffer large variations. The value of  $r(C_1$ — $C_7)$  and  $r(C_4$ — $C_7)$  is effectively the same for the three substituted norbornanes, with a slight increase for  $r(C_4$ — $C_7)$  with respect to norbornane, which breaks the symmetry in the bridge carbon parameters.

There is a remarkable consistency in the bond lengths values of the three substituted norbornanes fenchone, camphor, and camphene. The changes with respect to norbornane bond lengths follow the same trend and they focus on the six-membered ring because of the need of minimising ring strain after the introduction of an unsaturated substituent at  $C_2$ . The bond angles of the three substituted monoterpenoids also experience some variations with respect to norbornane, and mostly they vary in the same way. The largest change occurs for the  $\angle C_1C_2C_3$  angle, which increases by 3°–4° with respect to norbornane. Angle  $\angle C_2C_3C_4$  decreases by ca. 1%, while angles  $\angle C_1C_6C_5$  and  $\angle C_4C_5C_6$  are essentially the same considering their uncertainties. For the bond angles  $\angle C_3C_4C_5$  and  $\angle C_7C_1C_6$  the behavior of the camphor differs with respect to fenchone and camphene, which may be related to the different position of the methyl substituents, as indicated previously. Angle  $\angle C_3C_4C_5$  increases by ca. 1% for fenchone and camphene with respect to norbornane, while it decreases by ca. 2% for camphor. The opposite behavior is observed for angle  $\angle C_7C_1C_6$ . The angle involving the bridge carbon  $\angle C_1C_7C_4$  increases by ca. 1%–2% in the three norbornane derivatives but continues to be strained, with the largest value being 95.2(6)° for fenchone.

The structural adjustments in fenchone result in a twist in its six-membered ring such that the bonds  $C_2$ — $C_3$  and  $C_5$ — $C_6$  are not parallel like in norbornane (see Fig. 6). This twist has

been observed for camphor,<sup>16</sup> and has also been reported for other substituted norbornanes and camphanes, where it was tentatively related to the presence of a substituent in  $C_2$ .<sup>35</sup>

## V. CONCLUSIONS

The broadband rotational spectrum of fenchone has been observed for the first time and the rotational constants of the parent, all  $^{13}\text{C}$  and  $^{18}\text{O}$  species have been determined. Theoretical predictions with several density functional and *ab initio* methods and with different basis sets have been performed. All methods provide satisfactory values of the rotational constants. The best agreement between theory and experiment was provided by the MP2/6-311++G(d,p) level of theory, with differences of 0.3% or lower for the three rotational constants, followed by B3LYP with the cc-pVTZ and aug-cc-pVTZ basis sets, which perform similarly with differences between equilibrium and ground-state rotational constants lower than 0.5%.

The substitution and  $r_0$  structures of fenchone have been determined, and the latter has been compared with those previously reported for norbornane and the norbornane derivatives camphor and camphene, both with substituents at  $C_2$  like fenchone. The structure of fenchone is remarkably similar to those of camphor and camphene. Comparison with camphor allows identification of changes in  $\angle\text{CCC}$  angles due to the different position of the methyl groups. All norbornane derivatives display similar structural changes with respect to norbornane. These changes mainly affect the bond lengths and angles of the six-membered rings, indicating that the substituent at  $C_2$  drives structural adjustments to minimise ring strain after its introduction.

Rotational spectroscopy has demonstrated to be a powerful technique to determine molecular structure. The development of broadband rotational spectroscopy and the improved accessibility to lower frequency regions of the rotational spectrum makes it possible to tackle larger molecules.<sup>20,36,37</sup> In this context, the determination of the structure of fenchone will pave the way to study its complexes with water and other molecules, shedding light on the interactions that this molecule establishes in processes involving living organisms and the environment.

## SUPPLEMENTARY MATERIAL

See [supplementary material](#) for Tables S1–S12, with the observed frequencies and residuals for the rotational transitions of the parent and all observed isotopologues of fenchone; Table S13 with the substitution coordinates of the heavy atoms of fenchone; Figure S1, with the internal rotation barriers for the methyl groups of fenchone calculated at the MP2/6-311++G(d,p) level of theory.

## ACKNOWLEDGMENTS

This work was supported by the EU FP7 (Marie Curie Grant No. PCIG12-GA-2012-334525) and King's College London. The authors thank Professor J. L. Alonso

(Universidad de Valladolid, Spain) and his group, in particular S. Mata, for valuable discussions on the chirped pulsed technique.

- <sup>1</sup>G. Wang, W. Tang, and R. R. Bidigare, in *Natural Products: Drug Discovery and Therapeutic Medicine*, edited by L. Zhang and A. L. Demain (Humana Press Inc., Totowa, NJ, 2005), pp. 197–227.
- <sup>2</sup>P. K. Ajikumar, K. Tyo, S. Carlsen, O. Mucha, T. Heng Phon, and G. Stephanopoulos, *Mol. Pharm.* **5**, 167 (2008).
- <sup>3</sup>C. Sell, *The Chemistry of Fragrances*, 2nd ed. (RSC Publishing, 2006).
- <sup>4</sup>M. Hallquist *et al.*, *Atmos. Chem. Phys.* **9**, 5155 (2009).
- <sup>5</sup>R. Chizzola, in *Natural Products*, edited by K. G. Ramawat and J. M. Mérillon (Springer-Verlag Berlin, Heidelberg, 2013), pp. 2973–3008.
- <sup>6</sup>J. H. Krolla and J. H. Seinfeld, *Atmos. Environ.* **42**, 3593 (2008).
- <sup>7</sup>G. G. Brown, B. C. Dian, K. O. Douglass, S. M. Geyer, S. T. Shipman, and B. H. Pate, *Rev. Sci. Instrum.* **79**, 053193 (2008).
- <sup>8</sup>R. Kotan, S. Kordali, and A. Cakir, *Z. Naturforsch.* **62c**, 507 (2007).
- <sup>9</sup>A. S. Fouda, S. M. Rashwan, and H. A. Abo-Mosallam, *Desalin. Water Treat.* **52**, 5175 (2014).
- <sup>10</sup>A. A. Ceacero-Vega, B. Ballesteros, I. Bejan, I. Barnes, E. Jiménez, and J. Albaladejo, *J. Phys. Chem. A* **116**, 4097 (2012).
- <sup>11</sup>J. R. Avilés Moreno, T. R. Huet, and J. J. López González, *Struct. Chem.* **24**, 1163 (2013).
- <sup>12</sup>D. Schmitz, V. A. Shubert, B. M. Giuliano, and M. Schnell, *J. Chem. Phys.* **141**, 034304 (2014).
- <sup>13</sup>D. Schmitz, V. A. Shubert, T. Betz, and M. Schnell, *Front. Chem.* **3**, 15 (2015).
- <sup>14</sup>H. V. L. Nguyen, H. Mouhib, S. Klahm, W. Stahl, and I. Kleiner, *Phys. Chem. Chem. Phys.* **15**, 10012 (2013).
- <sup>15</sup>J. R. Avilés Moreno, F. Partal Ureña, J. J. López González, and T. R. Huet, *Chem. Phys. Lett.* **473**, 17 (2009), peryllaldehyde.
- <sup>16</sup>Z. Kisiel, O. Desyatnyk, E. Białkowska-Jaworska, and L. Pszczółkowski, *Phys. Chem. Chem. Phys.* **5**, 820 (2003).
- <sup>17</sup>E. M. Neeman, P. Dréan, and T. R. Huet, *J. Mol. Spectrosc.* **322**, 50 (2016).
- <sup>18</sup>S. Ghosh and S. Banerjee, *ARKIVOC* **vii**, 8 (2002).
- <sup>19</sup>D. Loru, I. Peña, J. L. Alonso, and M. E. Sanz, *Chem. Commun.* **52**, 3615 (2016).
- <sup>20</sup>N. A. Seifert, C. Pérez, J. L. Neill, B. H. Pate, M. Vallejo-López, A. Lesarri, E. J. Cocinero, and F. Castaño, *Phys. Chem. Chem. Phys.* **17**, 18282 (2015).
- <sup>21</sup>V. Vaquero, M. E. Sanz, J. C. López, and J. L. Alonso, *J. Phys. Chem. A* **111**, 3443 (2007).
- <sup>22</sup>C. Pérez, M. T. Muckle, D. P. Zaleski, N. A. Seifert, B. Temelso, G. C. Shields, Z. Kisiel, and B. H. Pate, *Science* **336**, 897 (2012).
- <sup>23</sup>A. D. Bond and J. E. Davies, *Acta Crystallogr., Sect. E: Struct. Rep. Online* **57**, o1034 (2001).
- <sup>24</sup>J. L. Neill, S. T. Shipman, L. Alvarez-Valtierra, A. Lesarri, Z. Kisiel, and B. H. Pate, *J. Mol. Spectrosc.* **269**, 21 (2011).
- <sup>25</sup>S. A. Cooke and P. Ohring, *J. Spectrosc.* 698392 (2013).
- <sup>26</sup>J. K. G. Watson, in *Vibrational Spectra and Structure*, edited by J. R. Durig (Elsevier, New York, 1977), Vol. 6, pp. 1–78.
- <sup>27</sup>H. M. Pickett, *J. Mol. Spectrosc.* **148**, 371 (1991).
- <sup>28</sup>H. Hartwig and H. Dreizler, *Z. Naturforsch., A: Phys. Sci.* **51**, 923 (1996).
- <sup>29</sup>J.-R. Aviles-Moreno, E. Neeman, and T. R. Huet, “Microwave spectroscopy of monoterpenes of atmospheric interest:  $\alpha$ -pinene,  $\beta$ -pinene, and nopinone,” in *International Symposium on Molecular Spectroscopy, Talk WJ14, Champaign-Urbana, USA* (2014).
- <sup>30</sup>J. Kraitichman, *Am. J. Phys.* **21**, 17 (1953).
- <sup>31</sup>Z. Kisiel, PROSPE—Programs for ROTational SPEctroscopy, <http://info.ifpan.edu.pl/~kisiel/prospe.htm>; accessed 1 February 2016.
- <sup>32</sup>C. C. Costain, *Trans. Am. Cryst. Assoc.* **2**, 157 (1966).
- <sup>33</sup>J. K. G. Watson, A. Roytburg, and W. Ulrich, *J. Mol. Spectrosc.* **196**, 102 (1999).
- <sup>34</sup>L. Doms *et al.*, *J. Am. Chem. Soc.* **105**, 158 (1983).
- <sup>35</sup>C. Altona and M. Sundaralingan, *J. Am. Chem. Soc.* **92**, 1995 (1970).
- <sup>36</sup>N. A. Seifert, A. L. Steber, J. L. Neill, C. Pérez, D. P. Zaleski, B. H. Pate, and A. Lesarri, *Phys. Chem. Chem. Phys.* **15**, 11468 (2013).
- <sup>37</sup>I. Peña, C. Cabezas, and J. L. Alonso, *Angew. Chem., Int. Ed.* **54**, 2991 (2015).